Alteration of gut microbiota in elderly postmenopausal women with osteoporosis

Yingjuan Li
Southeast University Zhongda Hospital
Guangjian Mu
Southeast University Zhongda Hospital
Binbin Ma
Southeast University Zhongda Hospital
Panpan Lu
Southeast University Zhongda Hospital
Haiquan Huang
Southeast University Zhongda Hospital
Liqun Ren
Southeast University Zhongda Hospital
Hui Chen
Southeast University Zhongda Hospital
Yunfeng Rui
Southeast University Zhongda Hospital
Jihong Zou
Southeast University Zhongda Hospital
Naifeng Liu (liunaifengnj@outlook.com)
Southeast University Zhongda Hospital https://orcid.org/0000-0002-4197-9150

Research article

Keywords: osteoporosis, gut microbiota, alteration

Posted Date: March 27th, 2020

DOI: https://doi.org/10.21203/rs.3.rs-19484/v1

Abstract

Osteoporosis is a common bone disorder worldwide and causes bone fragility and fracture. Gut microbiota colonizes the gastrointestinal tract, and is associated with bone metabolism and osteoporosis. In our study, the alteration of gut microbiota in osteoporosis and its effects on bone metabolism were investigated. A total of 36 elderly postmenopausal osteoporotic women and 12 healthy controls were recruited, and their fecal samples were collected for 16S rRNA gene sequencing of gut microbiota on Illumina MiSeq platform. The venous blood and urine samples were also collected to determine the biochemical indexes. There was no obvious difference in Alpha diversity in the experiment group and control group, while differential Beta diversity was observed. The Partial Least Squares Discriminant Analysis (PLS-DA) model and variable importance in projection (VIP) scores showed that the osteoporotic women and healthy controls had different genera of Erysipelotrichaceae , Rothia , and Eubacterium . The metabolic function prediction of gut microbiota indicated that the experiment group had 634 unique functional categories, while the control group had 13 unique functional categories. The biochemical measurement revealed that the osteoclast activity indexes including urine N-terminal telopeptides of type I collagen (NTX), serum NTX, and serum C-terminal telopeptides of type I collagen (CTX) in the experiment group were higher than those in the control group, indicating that the osteoclast activity in osteoporotic women was increased. In addition, the correlation analysis of microbial metabolism with phenotypes showed the pathways in the significant modules of magenta, red, pink, and yellow were positively correlated with urine phosphate, urine creatinine, urine creatinine, serum calcium and other biochemical indexes. Collectively, our study identified the different genera between postmenopausal osteoporotic women and healthy controls, which might be potential targets for the treatment of osteoporosis.

Introduction

Osteoporosis is a common bone disorder worldwide with the characteristics of low bone strength, degeneration of bone tissues, decreased bone mass (Coughlan and Dockery, 2014). It is known that osteoporosis results in increased bone fragility and high risk of fracture, which affects more than 200 million people worldwide and remains to be a societal problem of health (Minisola et al., 2017; Kastner et al., 2010). As an aging-related disease, osteoporosis is more frequent in the elderly, especially among postmenopausal women (Wei et al., 2016; Wang et al., 2013; Gallagher and Levine, 2011). Approximately 50% of women aged over 50 years will have osteoporotic fracture (Sambrook and Cooper, 2006). The risk factors consist of age, gender, race, and other factors which may disturb the balance between bone loss and bone formation (e.g., lack of oestrogen, serum calcium level alteration, prolonged use of glucocorticoids). Currently, drugs are the main treatment for osteoporosis, however, the curative effect is limited, accompanied by side effects and high costs (Wu et al., 2013). Thus, huge efforts have been devoted to explore novel and effective targets for the treatment of osteoporosis.

The gut microbiota denotes the microbes colonizing the gastrointestinal tract and consists of anaerobes, aerobes and facultative anaerobes (Xu et al., 2017). Acquired at birth, gut microbiota co-evolves with the

host and is recognized as an organ which influences the physiology of host through multiple approaches (Ley et al., 2008). Some researchers have found that the gut microbiota is involved in bone mass and metabolism, indicating that gut microbiota may be associated with osteoporosis. Sjögren K et al showed that gut microbiota played a regulatory role in bone mass by acting on the immune status and resorption of bone in mice (Sjögren et al., 2012). Charles JF et al revealed that gut microbiota acted as anabolic stimulus to the skeleton in mice and enhanced the formation and growth of bone (Yan et al., 2016). It was found that variations of the gut microbiome in mice could weaken the bone strength and tissue material properties (Guss et al., 2017). Pacifici R et al demonstrated that gut microbiota was associated with the bone loss in mice with sex steroid deficiency, which could be improved by probiotics (Li et al., 2016). Although the studies mentioned above have explained the relationship between gut microbiota and osteoporosis, they were all performed based on animal experiments. The researches on human might unfold the association between gut microbiota and osteoporosis more directly and convincingly.

Our study investigated the influence of gut microbiota on the bone metabolism and osteoporosis among the elderly postmenopausal women through analysis of gut microbiota by next-generation sequencing technology (NGS) and biochemical detection. We aimed to elucidate the distribution and composition of gut microbiota which contributed to the improvement of bone metabolism and osteoporosis, and further implicate the possibility and feasibility of gut microbiota as promising targets for the treatment of osteoporosis based on current research.

1 Materials And Methods

Ethics statement

This study was approved by the Ethics Committee of Zhongda Hospital Southeast University and performed according to the Declaration of Helsinki. Written informed consents were obtained from all participants.

Study subjects

A total of 36 elderly postmenopausal osteoporotic women (mean age: 74.42 ± 7.48) and 12 women without osteoporosis (mean age: 64.0 ± 4.86) were recruited as the experiment and control groups respectively. Bone mineral density (BMD, T-Score ≤ -2.5 SD) was used for diagnosis of osteoporosis according to the guidelines for the diagnosis and treatment of primary osteoporosis (Baum and Peters, 2008). The detailed clinical data for individual human subject was shown in Table S1.

Biochemical measurement

The venous blood and urine samples of patients in the experiment and control groups were collected. Then the indexes of bone metabolism including serum and urine calcium, serum and urine creatinine, serum and urine phosphate, serum 25-Hydroxy Vitamin D, serum and urine N- and C-terminal telopeptides

of type I collagen (CTX and NTX), serum osteocalcin, calcitonin, parathyroid hormone (PTH), urine microalbumin and urine creatinine were determined. The indexes above were analyzed by R software.

DNA extraction

The fecal samples were collected and stored at -80. Total DNA of the fecal samples was extracted using InviMag stool DNA kit (Invitek, Germany). The quality and quantity of DNA samples were detected by 0.8% agarose gel electrophoresis and NanoDrop spectrophotometer (Thermo, USA) respectively.

Sequencing of the V3 and V4 regions of 16S rRNA gene

The V3 and V4 regions of 16S rRNA gene were amplified using the Q5 high-fidelity DNA polymerase (New England Biolabs), and the number of amplification cycles was controlled to ensure the low amplification cycles and consistent amplification conditions. The PCR products were detected by 2% agarose gel electrophoresis and purified by gel extraction kit (AXYGEN, USA). The real-time quantitative polymerase chain reaction (RT-qPCR) was performed according to the instructions of Quant-iT PicoGreen dsDNA Assay Kit (Invitrogen, USA) on Microplate reader (BioTek, FLx800). Then the samples were mixed proportionally based on the sequencing requirements and RT-qPCR results. After preparation of the sequencing library of the V3 and V4 regions of 16S rRNA gene, the samples were sequenced using the Illumina MiSeq System (Illumina Inc., USA) with paired-end 300-bp reads (Ong et al., 2018).

Bioinformatics analysis of sequencing data

Quantitative Insights Into Microbial Ecology software (QIIME, v1.8.0, http://qiime.org/) was used to filter the sequencing data with the following criteria: the reads were longer than 150 bp; there was no fuzzy N base; reads with more than 8 continuous identical bases or 1 primer 5’ base mismatch were excluded. Chimera was removed by USEARCH (v5.2.236, http://www.drive5.com/usearch/), and the length distribution of reads was analyzed by R language.

We determined the operational taxonomic units (OTUs) using UCLUST with a similarity threshold of 97%, and selected the most abundant sequence of each OTU as the representative one. Alpha diversity was calculated by QIIME, and rarefaction, Chao1 index, and ACE index were calculated. The species accumulation curves were plotted using R software. Principal component analysis (PCA) was conducted using R software to analyze the Beta diversity. Partial Least Squares Discriminant Analysis (PLS-DA) model was constructed using R software and variable importance in projection (VIP) scores were calculated to screen the different genera between experiment and control groups. The metabolic function of microbiota was predicted by Phylogenetic Investigation of Communities by Reconstruction of Unobserved States (PICRUSt) and the species abundance of the original data was adjusted.

Weighted gene co-expression network analysis (WGCNA) was performed to analyze the correlation of microbial metabolism with phenotypes by using WGCNA R package. The abundance matrix of Kyoto Encyclopedia of Genes and Genomes (KEGG) pathways was used as input matrix, and the biochemical indexes were used as clinical information.

Statistical analysis

All data were expressed as mean ± standard deviation. Statistical analyses were performed using GraphPad Prism 6.0 statistical software (GraphPad Software Inc, La Jolla, CA, USA). Comparisons among multiple groups were accessed by two-way analysis of variance followed by Bonferroni test, while comparisons between two groups were evaluated by Student t test. p value < 0.05 was considered to indicate a statistically significant difference.

2 Results

Identification and classification of OTUs

To analyze the difference in gut microbiota between osteoporotic women and healthy controls, we collected their fecal samples and conducted the Illumina sequencing of the V3 and V4 regions of 16S rRNA gene. After removed the questioned sequences, the reads numbers were recorded (Table 1). We obtained 3,478 OTUs for the experiment group and 2,640 OTUs for the control group. There were 2,541 common OUTs between the two groups (Fig. 1B). The classifications of the samples were shown in Table 2 and Fig. 1A, and “Unclassified” denoted the OTU numbers that could not be classified into other unites.

Table 1
Reads numbers of the samples.

Sample	Reads_number
S0001	41700
S0002	54194
S0003	44963
S0004	52328
S0005	45591
S0006	46770
S0007	38273
S0008	40518
S0009	36657
S0010	48634
S0011	48072
S0012	56950
S0013	52674
S0014	44250
S0015	49192
S0016	50039
S0017	52047
S0018	48700
S0019	51009
S0020	49244
S0021	44448
S0022	56779
S0023	41626
S0024	52343
S0025	54557

Sample	Reads_number
S0026	42539
S0027	48829
S0028	43173
S0029	38803
S0030	51543
S0031	47267
S0032	43334
S0033	44484
S0034	48630
S0035	58980
S0036	48131
D0001	57172
D0002	51741
D0003	62540
D0004	46808
D0005	52189
D0006	53637
D0007	41287
D0008	53781
D0009	41666
D0010	41811
D0011	47329
D0012	49969
total	2317201

Table 2
The OTU numbers classified into each unite.

Sample	Phylum	Class	Order	Family	Genus	Species	Unclassified
S0001	796	796	794	723	435	102	0
S0002	732	732	732	677	393	124	0
S0003	837	837	837	780	447	110	0
S0004	261	261	261	257	191	89	0
S0005	687	687	687	639	402	69	0
S0006	409	409	408	382	271	67	0
S0007	662	662	662	615	378	119	0
S0008	816	816	816	736	426	89	0
S0009	675	675	674	627	372	100	0
S0010	602	602	602	568	352	73	0
S0011	480	480	480	448	240	40	0
S0012	608	608	605	535	334	94	0
S0013	439	439	438	411	189	58	0
S0014	338	338	336	323	191	63	0
S0015	547	547	543	524	277	61	0
S0016	437	437	435	417	281	82	0
S0017	553	553	553	508	272	49	0
S0018	492	492	492	466	267	96	0
S0019	371	371	371	324	167	47	0
S0020	504	504	504	485	284	73	0
S0021	651	651	651	586	310	123	0
S0022	622	622	622	579	366	105	0
S0023	502	502	501	491	296	77	0
S0024	458	458	458	436	321	95	0
S0025	522	522	520	494	292	106	0
S0026	725	725	725	678	309	109	0

Sample	Phylum	Class	Order	Family	Genus	Species	Unclassified
S0027	707	707	707	669	442	105	0
S0028	723	723	719	688	427	114	0
S0029	407	407	405	391	236	53	0
S0030	484	484	483	439	293	39	0
S0031	622	622	622	587	232	50	0
S0032	337	337	336	320	175	86	0
S0033	551	551	551	500	301	88	0
S0034	543	543	530	488	307	85	0
S0035	563	563	563	556	396	95	0
S0036	820	820	819	775	433	149	0
D0001	684	684	683	633	396	129	0
D0002	498	498	496	452	241	37	0
D0003	892	892	892	826	437	125	0
D0004	516	516	515	482	306	103	0
D0005	691	691	691	647	351	121	0
D0006	494	494	490	468	240	63	0
D0007	448	448	444	422	244	92	0
D0008	941	941	941	880	414	118	0
D0009	303	303	303	300	206	48	0
D0010	344	344	343	330	230	56	0
D0011	679	679	679	620	307	96	0
D0012	611	611	610	558	330	72	0

No obvious difference of Alpha diversity was observed in osteoporotic women and healthy controls

The rarefaction curves of the samples were plotted. As shown in Figure S1, the curves were flat, indicating that the OTU numbers did not increase significantly with the increase of sequencing depth, and the current sequencing depth was able to reflect the OTU number. The species accumulation curves of the samples were shown in Figure S2A. The result revealed that the species number did not significantly increase with the increase of sample size. Thus, the current sample size was able to reflect the

abundance of species. The rank abundance curves were plotted based on the OTU abundance of samples and shown in Figure S2B.

After calculation of Chao1 and ACE indexes, it was found that there was no significant difference in Chao1 and ACE indexes of the experiment and control groups (Table 3, Fig. 2, $p > 0.05$).

Table 3
The Chao1 and ACE indexes of samples.

Sample	Chao1	ACE
S0001	922.85	922.23
S0002	814.54	829.42
S0003	1015.14	1016.26
S0004	286.57	297.1
S0005	764.21	758.18
S0006	438.65	454.57
S0007	662	662
S0008	816	816
S0009	675	675
S0010	654.8	683.19
S0011	533.55	578.13
S0012	650.96	681.88
S0013	472.4	494.81
S0014	357.6	370.99
S0015	587.54	604.78
S0016	473.68	496.62
S0017	606	630.73
S0018	591.04	592.33
S0019	390.6	399.77
S0020	561.21	578.01
S0021	747.72	763.02
S0022	664.62	678.74
S0023	508.89	522.19
S0024	494.12	504.01
S0025	560.02	589.97

Sample	Chao1	ACE
S0026	885.12	871.56
S0027	803.57	818.75
S0028	828.23	893.53
S0029	458	449.14
S0030	515.67	535.77
S0031	678.65	706.53
S0032	420.27	393.92
S0033	606.1	620.32
S0034	571.59	584.43
S0035	605	633.05
S0036	964.44	959.6
D0001	768.46	803.27
D0002	528.96	537.23
D0003	966.52	1003.06
D0004	553.85	581.95
D0005	753.55	778.95
D0006	527.7	551.63
D0007	530.27	515.86
D0008	1028.37	1089.91
D0009	329	340.96
D0010	380.36	387.28
D0011	679	679
D0012	661	672.57

Difference in Beta diversity was observed between osteoporotic women and healthy controls

PCA was performed for Beta analysis by transforming OTU abundance matrix into two and three dimensional images. As shown in Figure S3, the long distance between the experiment group and control group suggested that the two groups had obviously distinct gut microbiota.

Differential microbiota between osteoporotic women and healthy controls

The PLS-DA model was constructed based on the data of species abundance and grouping. The top 20 different genera were selected after calculation of the VIP scores (Table 4). Among them, Erysipelotrichaceae, Rothia, and Eubacterium showed higher VIP scores, indicating that there were obvious differences in these genera between osteoporotic women and healthy controls. As shown in Figure S4, the long distance between blue dots and orange dots, which denoted the control group and experiment group respectively, suggested that this model could classify the samples accurately.

Table 4
The top 20 different genera between osteoporotic women and healthy controls.

No.	Genus	VIP
1	Erysipelotrichaceae	3.180635621
2	Rothia	2.486952771
3	Eubacterium	2.438032539
4	Ruminococcus	2.430350419
5	Oribacterium	2.423163595
6	Bulleidia	2.319810008
7	Faecalibacterium	2.279513599
8	Dorea	2.201598906
9	Citrobacter	2.187893876
10	Lactococcus	2.117118578
11	[Clostridium]	2.09903073
12	Leuconostoc	1.947476038
13	Aeromonadaceae	1.919289997
14	Granulicatella	1.831999696
15	Serratia	1.814243487
16	Bilophila	1.748321474
17	Roseburia	1.60388443
18	Enterobacter	1.59085035
19	Anaerotruncus	1.589144623
20	Mogibacterium	1.531936392

Metabolic function prediction of gut microbiota

PICRUSt was used to predict the KEGG functional categories of the microbiota. The relative abundance of KEGG functional categories in experiment and control groups were shown in Fig. 3A. Clustering analysis was performed on the top 50 functional categories with high abundance and the heatmap was shown in Fig. 3B. Then the common and unique function number of each group was calculated. As shown in

Fig. 3C, the experiment group had 634 unique functional categories, while the control group had 13 unique functional categories. There were 5,456 common functional categories between the two groups.

Osteoporotic women presented increased osteoclast activity

The biochemical indexes of serum and urine of experiment and control groups were measured. As shown in Fig. 4, the osteoclast activity indexes including urine NTX ($p < 0.05$), serum NTX, and serum CTX in the experiment group were higher than those in the control group. The results indicated that compared with healthy controls, the osteoclast activity in osteoporotic women was increased. In addition, the serum calcium in the control group was significantly higher than that in the experiment group ($P < 0.05$).

Correlation of microbial metabolism with biochemical indexes

The input matrix included 48 samples and 6,909 KEGG pathways. Clustering analysis of the samples showed that there were no outlier samples (Fig. 5). Soft-threshold was selected as $\beta = 16$ to ensure it met the criterion of scale-free network, with the correlation coefficient between log(k) and log(p(k)) greater than 0.85 (Fig. 6A). k represented the intramodular connectivity and p(k) represented the frequency distribution of the connectivity. After transformation from expression matrix to adjacency matrix, the adjacency matrix was transformed to topological matrix. Based on topological overlap measure (TOM), hierarchical clustering analysis was performed. Dynamic branch cutting method was adopted to identity different modules, and the module eigengene (ME) was calculated as the representative gene of each module. Clustering analysis on the modules was carried out, with the highly correlated modules merged (height = 0.25). A total of 10 modules were obtained, and the grey module represented the pathways that could not be clustered into other modules (Fig. 6B).

Based on the ME, the module-phenotype relationship was calculated. The information of phenotype was shown in Table 5. As shown in Fig. 6C, the magenta, red, pink, and yellow modules were positively correlated with urine phosphate, urine creatinine, urine creatinine, serum calcium (correlation coefficients: 0.31, 0.33, 0.36, 0.39; p values: 0.03, 0.02, 0.01, 0.007, respectively) and other biochemical indexes. The pathways in these significant modules ($N_{\text{magenta module}} = 113$; $N_{\text{red module}} = 153$; $N_{\text{pink module}} = 128$; $N_{\text{yellow module}} = 180$) were exported for further analysis on their relationship with biochemical indexes of osteoporosis (Table S2).

Table 5
The information of phenotype.

Phenotype	Variable type
Blood_Ca	Continuous variable
Blood_P4	Continuous variable
PTH	Continuous variable
OC	Continuous variable
Blood_NTX	Continuous variable
Blood_CTX	Continuous variable
VD	Continuous variable
Urinary_microalbumin	Continuous variable
Urinary_creatinine	Continuous variable
Urinary_NTX	Continuous variable
Urinary_CTX	Continuous variable
Calcitonin	Continuous variable
Urinary_Ca	Continuous variable
Urinary_P4	Continuous variable

3 Discussion

Osteoporosis, as an aging-related disease, affects many people and is considered as a societal problem of health (Kastner et al., 2010). Gut microbiota colonizes gastrointestinal tract and plays a key role in bone mass mediation through regulating several biological processes such as intestinal calcium absorption and osteoclastogenesis (Sjögren et al., 2012; Weaver and Connie, 2015; McCabe et al., 2015). In this study, we analyzed the gut microbiota in elderly postmenopausal osteoporotic women and healthy controls. The results showed that there was no obvious difference in Alpha diversity in the experiment group and control group, while Beta diversity showed significant difference. Moreover, the osteoporotic women and healthy controls had different genera of Erysipelotrichaceae, Rothia, and Eubacterium, indicating that these genera might be associated with the occurrence and development of osteoporosis.

Erysipelotrichaceae belongs to the Firmicutes phylum and is implicated in host physiology and diseases, such as metabolic disorders and gastrointestinal diseases (Kaakoush, 2010). It has been proved that Erysipelotrichaceae is associated with the lipid metabolism of the host (Martinez et al., 2013). The species of Erysipelotrichaceae presented a bloom in diet-induced obesity (Turnbaugh et al., 2008). Obese

people showed elevated Erysipelotrichaceae level, while the hamster with hypercholesterolemia had decreased Erysipelotrichaceae level after treatment (Zhang et al., 2009; Martinez et al., 2009). Fleissner CK et al. found that mice with high-fat or western diet showed higher Erysipelotrichaceae abundance (Fleissner et al., 2010). Besides, flavonoids, which were used for weight loss, could suppress the Erysipelotrichaceae growth (Hurt and Wilson, 2012; Etxeberria et al., 2015). On the other hand, accumulating evidence has proved that lipid metabolism is associated with BMD, the key diagnostic index of osteoporosis. Fluctuation of lipid level was found to be related with BMD alteration, while the treatment of hyperlipidemia could lead to elevated BMD (Tian and Yu, 2015). Mundy G et al showed application of statins, which were used to reduce serum cholesterol, could promote bone formation and might be helpful for the treatment of osteoporosis (Mundy, 1999). Kapitola J et al found women with osteoporosis and vertebral fractures showed increased cholesterol levels compared with the healthy controls (Broulik and Kapitola, 1993). Thus, we speculated that Erysipelotrichaceae might involve in osteoporosis via the lipid metabolism.

Rothia belongs to Gram-positive bacterium, and consists of several species: Rothia dentocariosa, Rothia mucilaginosa, Rothia nasimurium, Rothia aeria, Rothia amarae, Rothia endophytica and Rothia terrae (Tsuzukibashi et al., 2017). Although Rothia genus is the normal microbe of oropharynx and upper respiratory tract (Trivedi and Malhotra, 2013), it may cause infections of the host sometimes, such as meningitis, bacteremia, peritonitis, endophthalmitis and pneumonia (Ramanan et al., 2014). Eubacterium belongs to Firmicutes phylum and consists of diverse species (Kadam and Chuan, 2016). Karlsson FH et al analyzed the gut microbiota in atherosclerosis patients and healthy controls, and found that different Eubacterium abundance between the two groups (Karlsson et al., 2012). However, to our knowledge, the alterations of Rothia and Eubacterium abundance in osteoporosis were rarely reported. In addition, among the three different genera between osteoporotic patients and healthy controls of our study, both Erysipelotrichaceae and Eubacterium belong to the Firmicutes phylum. Ji YH el al analyzed the gut microbiota in osteoporosis patients and found that Firmicutes showed distinct proportion between osteoporosis patients and negative controls (Wang et al., 2017), which was consistent with our study. These results also indicated that Firmicutes phylum might be potential osteoporosis-related phylum.

In conclusion, our study identified the different genera between postmenopausal osteoporotic women and healthy controls, including Erysipelotrichaceae, Rothia, and Eubacterium. They might be potential targets for osteoporosis. However, further study on the specific effects of these genera on osteoporosis is needed to implicate the possibility and feasibility of them as promising targets for osteoporosis treatment.

Declarations

Acknowledgements

Not Applicable.

Abbreviations

Not Applicable.

Availability of data and material

All data generated or analyzed during this study are included in this published article.

Authors' contributions

All authors have read and approved the manuscript. LYJ made substantial contributions to conception and design, acquisition of data, analysis and interpretation of data; MGJ, MBB and LPP performed the experiments; HHQ and RLQ have been involved in drafting the manuscript or revising it critically for important intellectual content; CH and RYF given final approval of the version to be published. ZJH and LNF agreed to be accountable for all aspects of the work in ensuring that questions related to the accuracy or integrity of any part of the work are appropriately investigated and resolved.

Competing interests: All authors declare that they have no conflict of interest.

References

Baum, E., and Peters, K.M. (2008). The diagnosis and treatment of primary osteoporosis according to current guidelines. Deutsches Ärzteblatt International **105**, 573-81.

Broulik, P.D., and Kapitola, J. (1993). Interrelations between body weight, cigarette smoking and spine mineral density in osteoporotic czech women. Endocr Regul **27**, 57-60.

Coughlan, T., and Dockery, F. (2014). Osteoporosis and fracture risk in older people. Clinical Medicine **14**, 187-191.

Etxeberria, U., Arias, N., Boqué, N., Macarulla, M. T., Portillo, M. P., Martínez, J.A., et al. (2015). Reshaping faecal gut microbiota composition by the intake of trans-resveratrol and quercetin in high-fat sucrose diet-fed rats. The Journal of Nutritional Biochemistry **26**, 651-660.

Fleissner, C. K., Huebel, N., Abd El-Bary, M. M., Loh, G., Klaus, S., and Blaut, M. (2010). Absence of intestinal microbiota does not protect mice from diet-induced obesity. British Journal of Nutrition **104**, 919-929.

Gallagher, J.C., and Levine, J.P. (2011). Preventing osteoporosis in symptomatic postmenopausal women. Menopause **18**, 109-118.

Guss, J.D., Horsfield, M.W., Fontenele, F.F., Sandoval, T.N., Luna, M., Apoorva, F., et al. (2017). Alterations to the gut microbiome impair bone strength and tissue material properties. Journal of Bone and Mineral Research **32**, 1343-1353.

Hurt, R.T., and Wilson, T. (2012). Geriatric obesity: evaluating the evidence for the use of flavonoids to promote weight loss. Journal of Nutrition in Gerontology and Geriatrics **31**, 269-289.

Kaakoush, N.O. (2015). Insights into the role of erysipelotrichaceae in the human host. Frontiers in Cellular and Infection Microbiology **5**, 84.

Kadam, P.D., and Chuan, H.H. (2016). Erratum to: rectocutaneous fistula with transmigration of the suture: a rare delayed complication of vault fixation with the sacrospinous ligament. International Urogynecology Journal **27**, 505.

Karlsson, F.H., Fåk, F., Nookaew, I., Tremaroli, V., Fagerberg, B., Petranovic, D., et al. (2012). Symptomatic atherosclerosis is associated with an altered gut metagenome. Nature Communications **3**, 1245.

Kastner, M., Li, J., Lottridge, D., Marquez, C., Newton, D., and Straus, S. E. (2010). Development of a prototype clinical decision support tool for osteoporosis disease management: a qualitative study of focus groups. BMC Medical Informatics and Decision Making **10**, 40.

Ley, R.E., Hamady, M., Lozupone, C., Turnbaugh, P.J., Ramey, R.R., Bircher, J.S., et al. (2008). Evolution of mammals and their gut microbes **320**, 1647-1651.

Li, J.Y., Chassaing, B., Tyagi, A.M., Vaccaro, C., Luo, T., and Adams, J. (2016). Sex steroid deficiency-associated bone loss is microbiota dependent and prevented by probiotics. J Clin Invest **126**, 2049-2063.

Martinez, I., Perdicaro, D.J., Brown, A.W., Hammons, S., Carden, T.J., Carr, T.P., et al. (2013). Diet-induced alterations of host cholesterol metabolism are likely to affect the gut microbiota composition in hamsters. Applied and Environmental Microbiology **79**, 516-524.

Martinez, I., Wallace, G., Zhang, C., Legge, R., Benson, A.K., Carr, T.P., et al. (2009). Diet-induced metabolic improvements in a hamster model of hypercholesterolemia are strongly linked to alterations of the gut microbiota. Applied and Environmental Microbiology **75**, 4175-4184.

McCabe, L., Britton, R.A., and Parameswaran, N. (2015). Prebiotic and probiotic regulation of bone health: role of the intestine and its microbiome. Current Osteoporosis Reports **13**, 363-371.

Minisola, S., Cipriani, C., Occhiuto, M., and Pepe, J. (2017). New anabolic therapies for osteoporosis. Internal and Emergency Medicine **12**, 915-921.

Mundy, G. (1999). Stimulation of bone formation in vitro and in rodents by statins. Science **286**, 1946-1949

Tong, X., Xu, J., Lian, F., Yu, X., Zhao, Y., and Xu, L. (2018). Structural Alteration of Gut Microbiota during the Amelioration of Human Type 2 Diabetes with Hyperlipidemia by Metformin and a Traditional Chinese Herbal Formula: a Multicenter, Randomized, Open Label Clinical Trial. MBio **9**, e02392-17

Ramanan, P., Barreto, J.N., Osmon, D.R., Tosh, P.K., and Diekema, D.J. (2014). Rothia bacteremia: a 10-year experience at mayo clinic, rochester, minnesota. Journal of Clinical Microbiology **52**, 3184-3189

Sambrook, P., and Cooper, C. (2006). Osteoporosis. Lancet **367**, 2010-2018

Sjögren, K., Engdahl, C., Henning, P., Lerner, U.H., Tremaroli, V., Lagerquist, M.K., et al. (2012). The gut microbiota regulates bone mass in mice. Journal of bone and mineral research **27**, 1357-1367.

Tian, L., and Yu, X. (2015). Lipid metabolism disorders and bone dysfunction–interrelated and mutually regulated (review). Molecular Medicine Reports **12**, 783-794

Trivedi, M.N., and Malhotra, P. (2013). Rothia prosthetic knee joint infection. Journal of Microbiology, Immunology and Infection **48**, 453-455

Tsuzukibashi, O., Uchibori, S., Kobayashi, T., Umezawa, K., Mashimo, C., Nambu, T., et al. (2017). Isolation and identification methods of rothia species in oral cavities. Journal of Microbiological Methods **134**, 21-26.

Turnbaugh, P.J., Bäckhed, F., Fulton, L., and Gordon, J.I. (2008). Diet-induced obesity is linked to marked but reversible alterations in the mouse distal gut microbiome. Cell Host & Microbe **3**, 213-223.

Wang, L., Shawn, Tracy, C., Moineddin, R., Upshur, R.E.G. (2013). Osteoporosis prescribing trends in primary care: a population-based retrospective cohort study. Primary Health Care Research & Development **14**, 1-6

Wang, J., Wang, Y., Gao, W., Wang, B., Zhao, H., and Zeng, Y. (2017). Diversity analysis of gut microbiota in osteoporosis and osteopenia patients. PeerJ 5:e3450

Weaver, Connie M (2015) Diet, gut microbiome, and bone health. Current Osteoporosis Reports **13**, 125-130

Wei, D., Jung, J., Yang, H., Stout, D.A., and Yang, L. (2016). Nanotechnology Treatment Options for Osteoporosis and Its Corresponding Consequences. Curr Osteoporos Rep **14**, 239-247

Wu, X., Guo, S., Shen, G., Ma, X., Tang, C., Xie, K., et al. (2013). Screening of osteoprotegerin-related feature genes in osteoporosis and functional analysis with dna microarray. Eur J Med Res **18**, 15.

Xu, X., Jia, X., Mo, L., Liu, C., Zheng, L., Yuan, Q., et al. (2017). Intestinal microbiota:a potential target for the treatment of postmenopausal osteoporosis. Bone Res **5**, 17046.

Yan, J., Herzog, J.W., Tsang, K., Brennan, C.A., Bower, M.A., Garrett, W.S., et al. (2016). Gut microbiota induce igf-1 and promote bone formation and growth. Proceedings of the National Academy of Sciences **113**, E7554-E7563.

Zhang, H., Dibaise, J.K., Zuccolo, A., Kudrna, D., Braidotti, M., Yu, Y., et al. (2009). Human gut microbiota in obesity and after gastric bypass. Proceedings of the National Academy of Sciences **106**, 2365-2370.

Supplemental Material

Figure S1. Rarefaction curves of the samples. The OTU number did not obviously increase with the increased depth of sequencing, and the sequencing depth was able to reflect the OTU number.

Figure S2. The species accumulation curve and rank abundance curve. (A) The number of species did not obviously increase with the increase of sample number. (B) The rank abundance curve of samples.

Figure S3. The osteoporotic women and healthy controls had significantly distinct gut microbiota. (A) The two dimensional image of PCA. (B) The three dimensional image of PCA.

Figure S4. The PLS-DA model could classify the samples accurately. The blue dots represented healthy controls and orange dots represented women with osteoporosis.

Figures

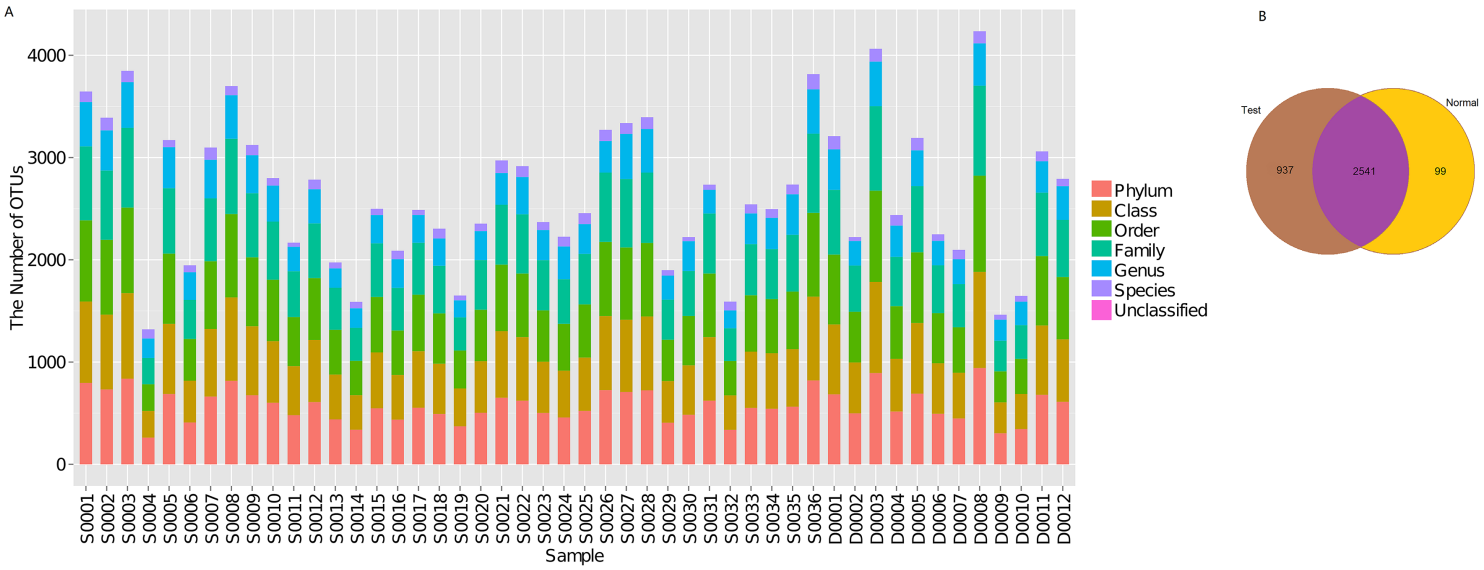

Figure 1

Identification and classification of OTUs. (A) The OTU numbers classified into each unite. (B) A total of 3,478 OTUs and 2,640 OTUs were identified for the experiment group and control group respectively. There were 2,541 common OUTs between the two groups.

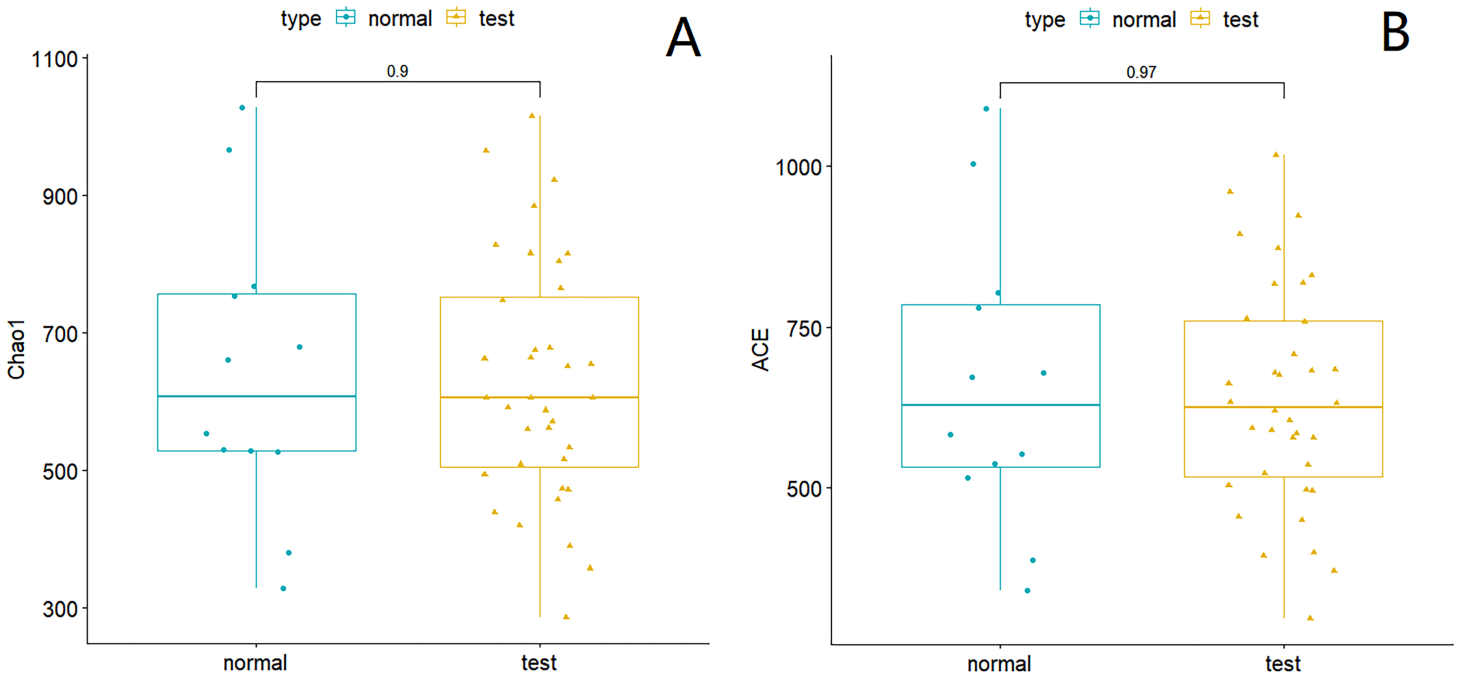

Figure 2

No significant difference in Chao1 and ACE indexes was observed in the experiment and control groups. (A) The Chao1 index of the experiment and control groups. (B) The ACE index of the experiment and control groups.

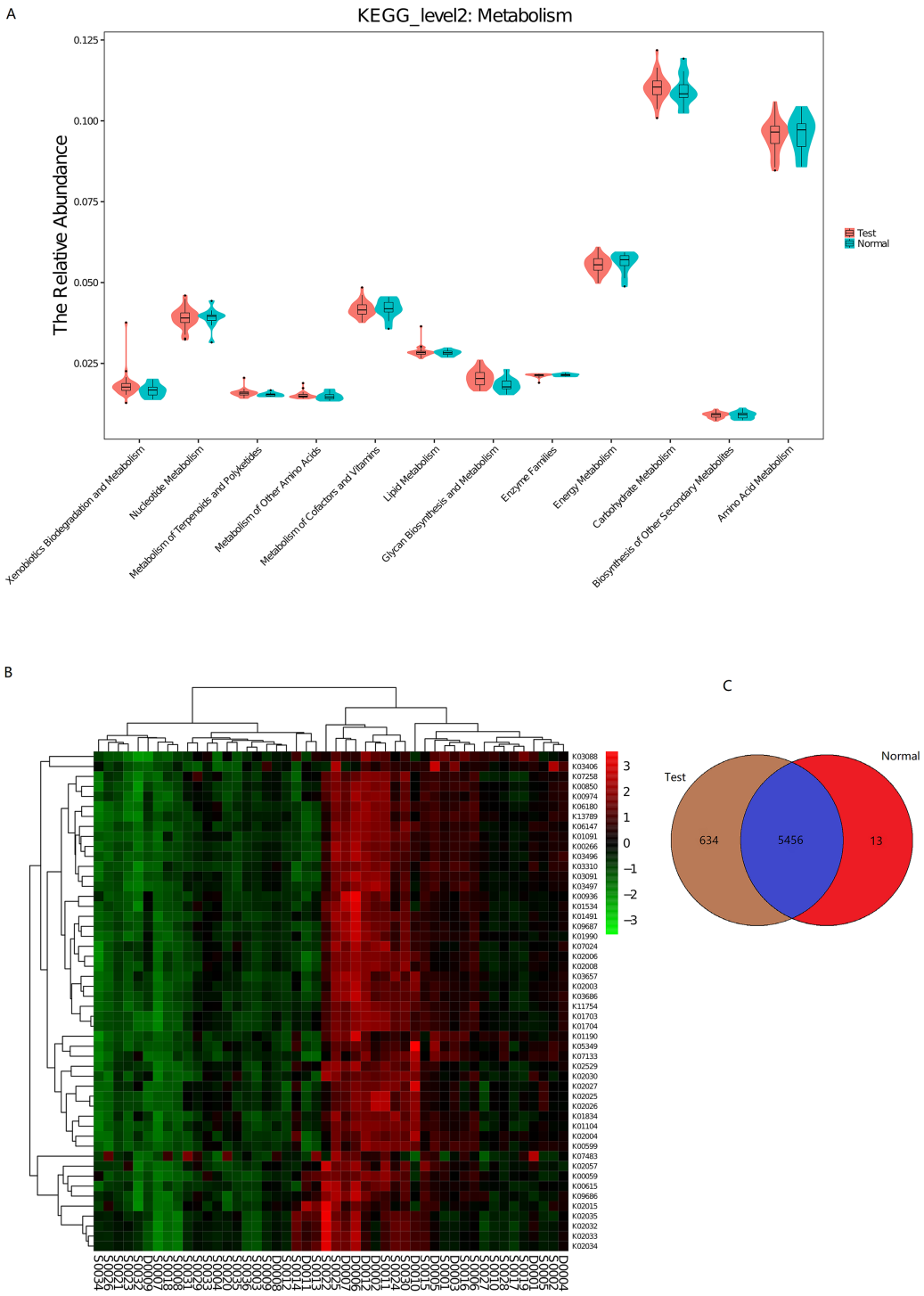

Figure 3

Metabolic function prediction of gut microbiota. (A) The relative abundance of KEGG functional categories in experiment and control groups. (B) Heatmap of top 50 functional categories with high abundance. (C) The common and unique metabolic functions of experiment and control groups.

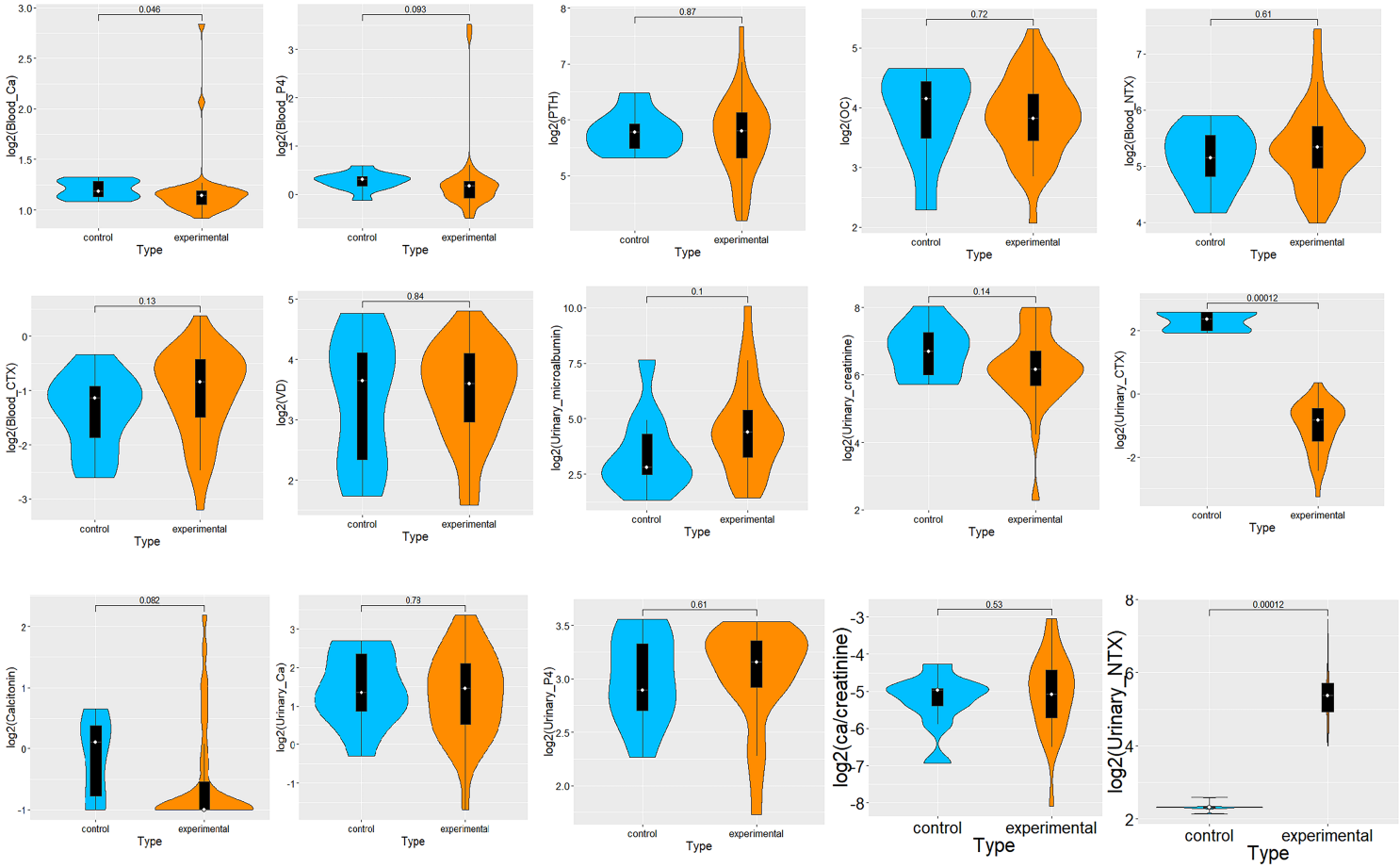

Figure 4

The biochemical indexes in serum and urine of experiment and control groups (serum calcium, serum phosphate, parathyroid hormone (PTH), osteocalcin, serum N-terminal telopeptides of type I collagen (NTX), serum C-terminal telopeptides of type I collagen (CTX), Vitamin D, urine microalbumin, urine creatinine, urine CTX, calcitonin, urine calcium, urine phosphate, blood creatinine, and urine NTX). The osteoclast activity indexes including urine NTX ($p < 0.05$), serum NTX, and serum CTX in the experiment group were higher than those in the control group, while the serum calcium in the control group was significantly higher than that in the experiment group ($p < 0.05$).

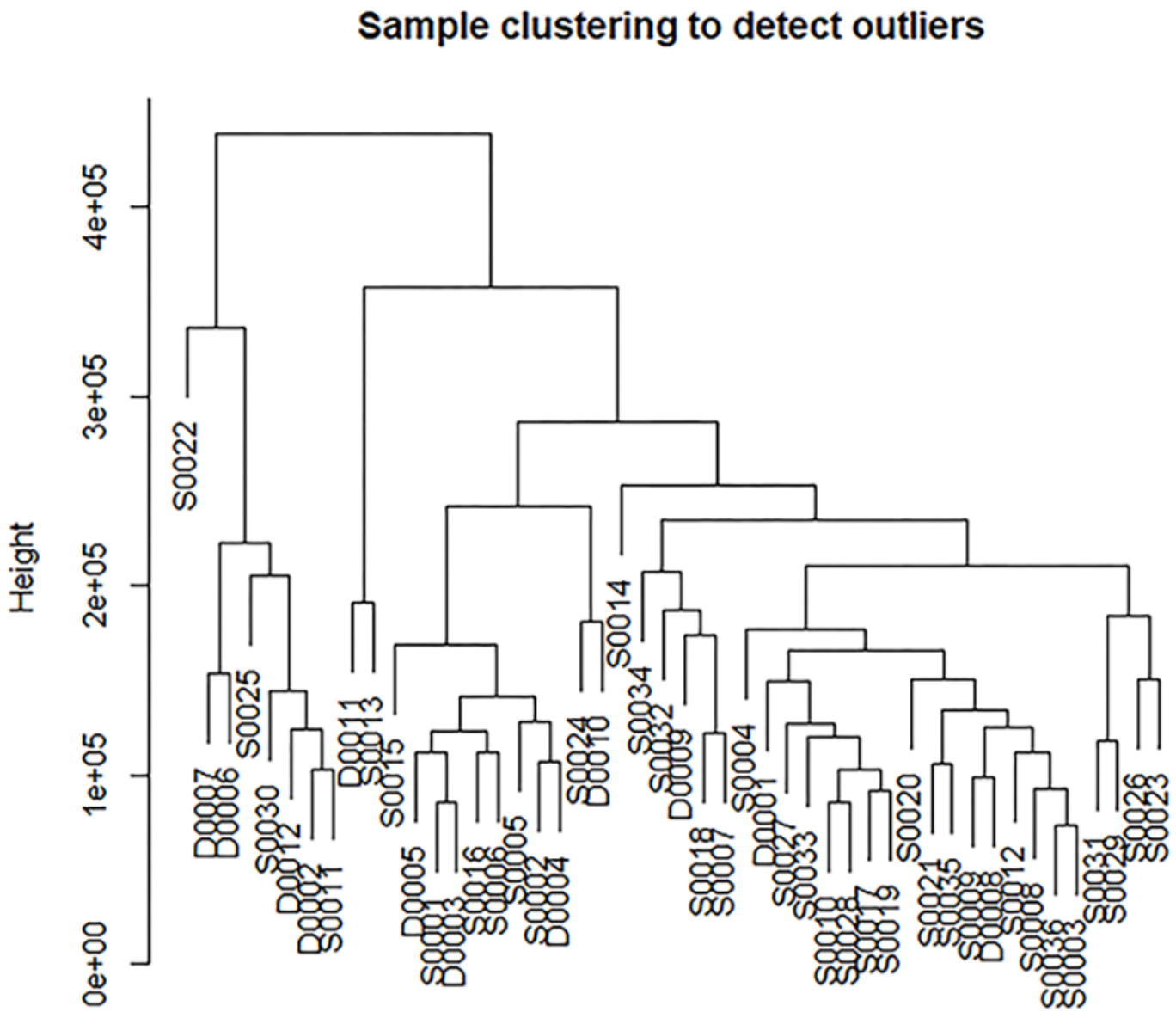

Figure 5

Clustering analysis of the samples showed there were no outlier samples.

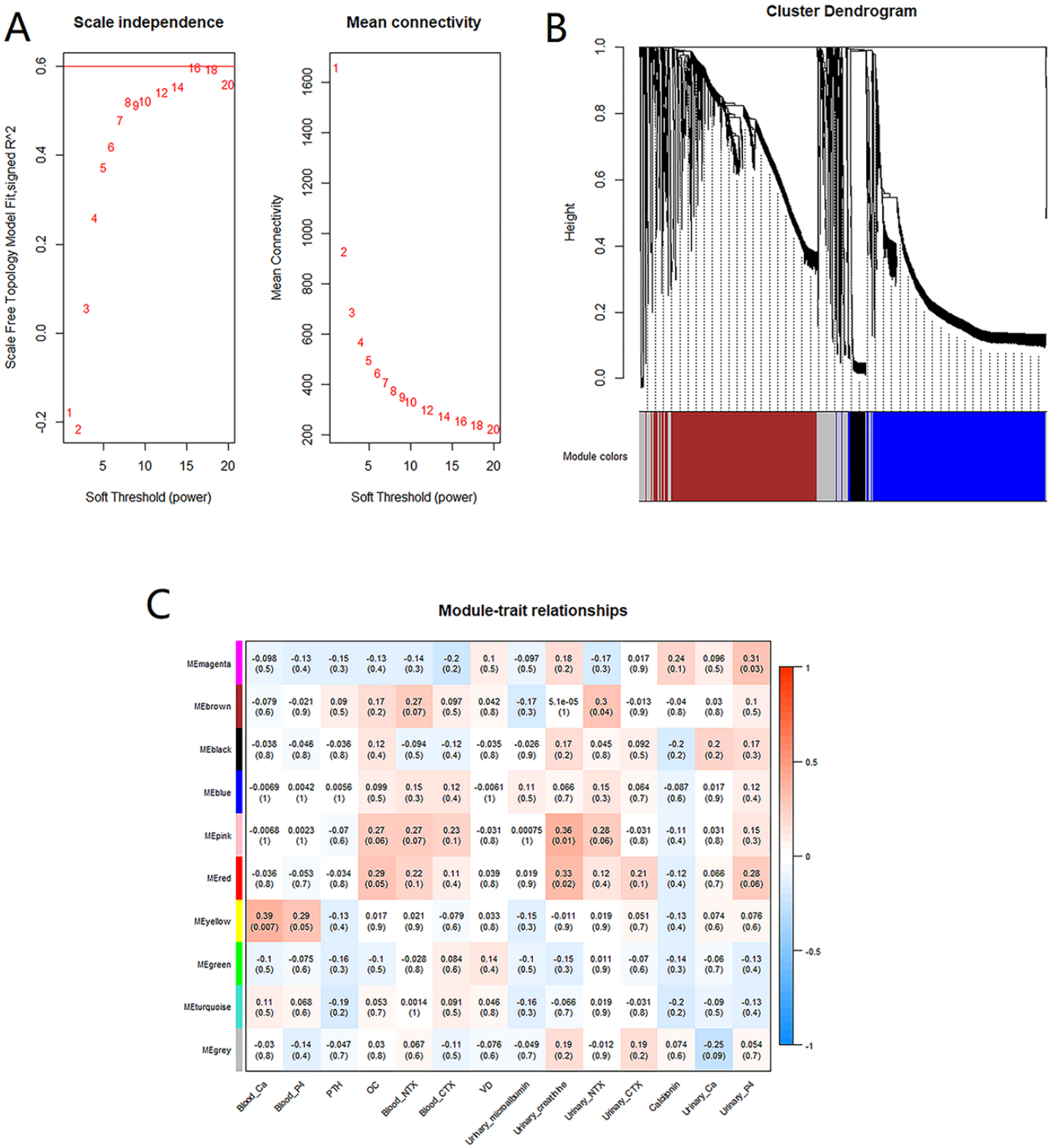

Figure 6

Correlation of microbial metabolism with biochemical indexes. (A) The soft-threshold was selected as β = 16 to meet the criteria of scale free topology. (B) Gene dendrogram showed 10 modules were identified and labeled by different colors. Pathways that couldn't be grouped into other modules were placed in the grey module. (C) Correlations analysis between modules and phenotypes showed the magenta, red, pink,

yellow modules were positively correlated with urine phosphate, urine creatinine, urine creatinine, serum calcium and other biochemical indexes.

Supplementary Files

This is a list of supplementary files associated with this preprint. Click to download.

- FigS4.png
- FigS3.tif
- FigS2.tif
- TableS1.xlsx
- FigS1.tif
- TableS2.xlsx